Front. Optoelectron. 2018, 11(4): 400–406
https://doi.org/10.1007/s12200-018-0851-8

RESEARCH ARTICLE

Temperature dependence simulation and characterization for InP/InGaAs avalanche photodiodes

Yanli ZHAO (✉)[1], Junjie TU[1], Jingjing XIANG[1,3], Ke WEN[1], Jing XU[1], Yang TIAN[1], Qiang LI[1], Yuchong TIAN[1], Runqi WANG[1], Wenyang LI[1], Mingwei GUO[1], Zhifeng LIU[2], Qi TANG[2]

1 Wuhan National Laboratory for Optoelectronics, Huazhong University of Science and Technology, Wuhan 430074, China
2 Wuhan Aroptics-Tech Co., LTD, Wuhan 430074, China
3 Sichuan Branch, China Unicom Network Communications Co., Ltd, Chengdu 610041, China

© Higher Education Press and Springer-Verlag GmbH Germany, part of Springer Nature 2018

Abstract Based on the newly proposed temperature dependent dead space model, the breakdown voltage and bandwidth of InP/InGaAs avalanche photodiode (APD) have been investigated in the temperature range from −50°C to 100°C. It was demonstrated that our proposed model is consistent with the experimental results. Our work may provide a guidance to the design of APDs with controllably low temperature coefficient.

Keywords optical communication, separate absorption, grading, charge, and multiplication avalanche photodiode (SAGCM APD), dead space effect, temperature coefficient

1 Introduction

InP/InGaAs separate absorption, grading, charge, and multiplication avalanche photodiodes (SAGCM APDs) have been widely applied in optics communication systems [1]. Moreover, there continues to be a strong interest in the application of the APD in the fields of quantum key distribution (QKD), national defense, and astrosurveillance, as so-called single photon avalanche diodes (SPADs) used in Geiger mode [2–6]. It is fascinating to notice that the design philosophy of APDs for the optical communication systems and that of SPADs for the quantum information applications, especially the QKD systems, are quite different [7]. Nevertheless, there is no doubt that the temperature dependence characteristics are crucial for APDs applied in the field of traditional optical communication, as well as SPADs in quantum communication systems. From the point of view of application, APDs immune to the change of temperature, i.e., APDs with low temperature coefficient is strongly designed, which has been drawn a lot of attention in recent years [8–11]. An empirical equation for temperature coefficient of APD was first reported in 1997 [8], but without considering the dead space effect. A simplified approach to time-domain modeling of avalanche photodiodes considering the dead space effect was reported in 1998 [9]. And then an improved empirical formula was proposed in 2010 [11].

In this work, based on static Poisson's equation and carrier transport equation, we developed a temperature dependent model for APDs taking dead space effect into account. A comparison of simulation with experimental results for the breakdown voltage and bandwidth of InP/InGaAs APD has been performed in the temperature range from −50°C to 100°C. It is shown that the temperature dependent dead space model is consistent with the measurements. Our work may provide a guidance to the design of APDs with controllably low temperature coefficient.

2 Physical model

The physical model was derived in the frequency domain by taking the Laplace transform of the current continuity equations, and the detail can be found in our previous work [12]. For the region without ionization (e.g., absorption layer, charge layer and grading layer), the analytic expression of carrier density can be derived according to the boundary conditions and the carrier transport equations. While for the multiplication layer, the avalanche region was divided into a number of spatial segments with equal energy spacing and the discrete expression can be deduced. Due to the dead space effect, it is thought that carriers must travel a fixed number of segments before

Received May 29, 2018; accepted September 20, 2018

E-mail: yanlizhao@hust.edu.cn

Special Issue—Energy Optoelectronics

reaching the threshold energy. Therefore, the carriers can be divided into two types: 1) carriers with energy lower than their ionization threshold, which cannot ionize; 2) carriers with energy above their threshold, which can ionize. For simplicity, as our previous report [12], it is assumed that the excess energy after ionization is zero, which means that, after ionization, three carriers (including the initial one carrier and the second electron and hole) with zero initial energy will be accelerated by electric field to reach the threshold energy and then ionize again. The carriers in the multiplication region are identified both by their space position and energy state.

The total current density J in the APD is calculated by

$$J = q\frac{(Sv)_n + (Sv)_p}{L}, \tag{1}$$

where q is the electronic charge, L is the thickness of the depletion region in APD. For the reach through type APD, $L = x_{\mathrm{m}} + x_{\mathrm{c}} + x_{\mathrm{g1}} + x_{\mathrm{a}}$, where x_{m}, x_{c}, x_{g1} and x_{a} are the thickness for multiplication layer, charge layer, grading layer and absorption layer, as shown in Fig. 1. In Fig. 1, the electric field distribution is also demonstrated, which was calculated from static Poisson's equation, as shown in our previous work [13]. $(Sv)_n$ indicates the product of the integration of electron density over the thickness L and the velocity of electrons. Similarly, $(Sv)_p$ represents the corresponding product of holes. The detailed expression for $S_n(S_p)$ can be found in the following part, i.e., $S_n(S_p) = S_{N\mathrm{m}}(S_{p\mathrm{m}}) + S_{N\mathrm{cg}}(S_{P\mathrm{cg}}) + S_{N\mathrm{ab}}(S_{P\mathrm{ab}})$, and the details can be found in the following part.

Assuming that the absorption layer is completely depleted, electrons and holes move with saturation velocities, and there is no recombination, the current continuity equations for electrons and holes are given by

$$\partial n(x,t)/\partial t + v_{n1}\{\partial n(x,t)/\partial x\} = g, \tag{2}$$

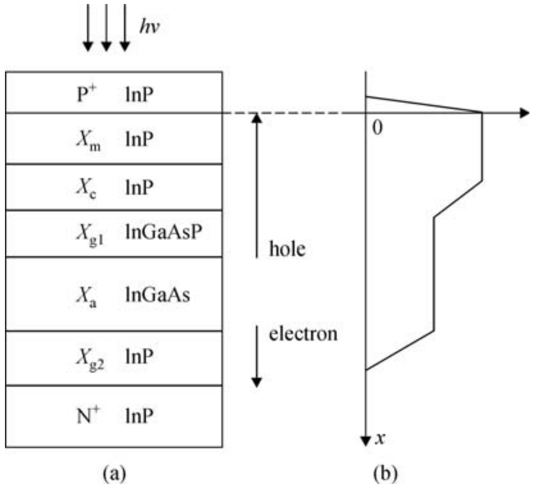

Fig. 1 Schematic structure of a InP/InGaAs SAGCM APD as well as its corresponding electric field distribution

$$\partial p(x,t)/\partial t - v_{p1}\{\partial p(x,t)/\partial x\} = g, \tag{3}$$

where $v_{n1}(v_{p1})$ is the saturation velocity of electrons (holes), n (p) is the volume density of electrons(holes), and g is the generation rate of electron-hole pairs. Under the lateral illumination condition, the generation rate g can be given by the spatial distribution, $g = g_0\delta(t)[1-\exp(-rx_{\mathrm{a}})]$ [14], where g_0 is the number of photons incident per unit distance, r is the absorption coefficient of the absorption region, x_{a} is the length of the absorption layer. Taking the Laplace transform of Eqs. (2) and (3), we obtain that

$$\frac{\partial N(x,s)}{\partial x} + \frac{s}{v_{n1}}N(x,s) = \frac{g_0}{v_{n1}}, \tag{4}$$

$$\frac{\partial P(x,s)}{\partial x} - \frac{s}{v_{p1}}P(x,s) = -\frac{g_0}{v_{p1}}. \tag{5}$$

According to the boundary conditions $N(x_0,s) = 0$, $P(x_0 + x_{\mathrm{a}},s) = 0$ and $x_0 = x_{\mathrm{m}} + x_{\mathrm{c}} + x_{\mathrm{g1}}$. The expressions of carrier density are given by

$$N(x,s) = \frac{g_0}{s}[1-\exp(-s(x-x_0)/v_{n1})], \tag{6}$$

$$P(x,s) = \frac{g_0}{s}[1-\exp(-s(x_0 + x_{\mathrm{a}}-x)/v_{p1})]. \tag{7}$$

To calculate holes and the electron's contribution to the current density, $N(x,s)$ (or $P(x,s)$), is integrated over the length of the absorption layer. Therefore, we obtain that

$$S_{N_{\mathrm{ab}}}(x_{\mathrm{a}},s) = \int_{x_0}^{x_0+x_{\mathrm{a}}} N(x,s)\mathrm{d}x = \frac{g_0}{s}\{x_{\mathrm{a}} + v_{n1}\{\exp(-sx_{\mathrm{a}}/v_{n1})-1\}/s\}, \tag{8}$$

$$S_{P_{\mathrm{ab}}}(x_{\mathrm{a}},s) = \int_{x_0}^{x_0+x_{\mathrm{a}}} P(x,s)\mathrm{d}x = \frac{g_0}{s}\{x_{\mathrm{a}}-v_{p1}\{1-\exp(-sx_{\mathrm{a}}/v_{p1})\}/s\}. \tag{9}$$

In the charge and grading layers, there is only carrier drift, no contribution from absorption of photons and without any impact ionization of carriers due to low electric field. Taking the Laplace transform of the current continuity equations, we obtain that

$$\frac{\partial N(x,s)}{\partial x} + \frac{s}{v_{n1}}N(x,s) = 0, \tag{10}$$

$$\frac{\partial P(x,s)}{\partial x} - \frac{s}{v_{p1}}P(x,s) = 0. \tag{11}$$

If electrons move a distance l from the location x, the carrier density in frequency domain shows a delay. Therefore, we obtain that

$$N(x+l,s)=N(x,s)\exp\left(-\frac{s}{v_{n1}}l\right),\tag{12}$$

$$P(x-l,s)=P(x,s)\exp\left(-\frac{s}{v_{p1}}l\right).\tag{13}$$

The sum of the carrier density in the charge and grading layers are given by

$$S_{P_{\rm cg}}(x_{\rm cg},s)=P(x_0,s)\frac{v_{p1}}{s}\left\{1-\exp\left(-\frac{s}{v_{p1}}(x_{\rm c}+x_{\rm g1})\right)\right\},\tag{14}$$

$$S_{N_{\rm cg}}(x_{\rm cg},s)=N(x_{\rm m},s)\frac{v_{n1}}{s}\left\{1-\exp\left(-\frac{s}{v_{n1}}(x_{\rm c}+x_{\rm g1}+x_{\rm a})\right)\right\},\tag{15}$$

where $N(x_{\rm m},s)$ is the electron density at position $x_{\rm m}$, and the detailed expression for $N(x_{\rm m},s)$ can be found in the following part. And $P(x_0,s)$ is the hole density at position x_0, which is given by the following equation

$$P\ \ (x_0,s)=\frac{g_0}{s}[1-\exp(-sx_{\rm a}/v_{p1})].\tag{16}$$

Similarly, for holes, $P(x_{\rm m},s)$ is the density of holes arriving at the boundary of the multiplication layer, and is given by

$$P(x_{\rm m},s)=P(x_0,s)\exp\left(-\frac{s}{v_{p1}}(x_{\rm c}+x_{\rm g1})\right).\tag{17}$$

The electric field in the multiplication layer is high enough to make carriers ionize, where the electrons and holes must satisfy the current continuity equations

$$\partial n(x,t)/\partial t+v_n\{\partial n(x,t)/\partial x\}$$
$$=\alpha n_{\rm e}(x,t)v_n+\beta p_{\rm e}(x,t)v_p,\tag{18}$$

$$\partial p(x,t)/\partial t-v_p\{\partial p(x,t)/\partial x\}$$
$$=\alpha n_{\rm e}(x,t)v_n+\beta p_{\rm e}(x,t)v_p,\tag{19}$$

where v_n (or v_p) is the saturation velocity of electrons (or holes) in the multiplication layer, α (or β) is the ionization coefficient of electrons (or holes), and $n_{\rm e}(x,t)$ (or $p_{\rm e}(x,t)$) are the electrons (or holes) (per unit volume) capable of initiating impact ionization. Taking the Laplace transform of Eqs. (18) and (19), we obtain that

$$\frac{\partial N(x,s)}{\partial x}+\frac{s}{v_n}N(x,s)$$
$$=\frac{1}{v_n}[\alpha N_{\rm e}(x,t)v_n+\beta P_{\rm e}(x,t)v_p],\tag{20}$$

$$\frac{\partial P(x,s)}{\partial x}-\frac{s}{v_p}P(x,s)$$
$$=-\frac{1}{v_p}[\alpha N_{\rm e}(x,s)v_n+\beta P_{\rm e}(x,s)v_p].\tag{21}$$

The avalanche region is divided into a number of spatial segments with equal energy spacing, and the carriers are divided into two types: 1) carriers with energy below their ionization threshold, 2) carriers with energy above their threshold. And the relation between the whole carriers and the carriers which can ionize in one spatial segment are shown that

$$\begin{aligned}P(x,s)&=P(x+\Delta x)\exp(-s\Delta x/v_p)\\&+P_{\rm e}(x+\Delta x)\exp(-s\Delta x/v_p)\\&\times\{1-\exp(-\beta\Delta x)\}\\&+\alpha v_nN_{\rm e}(x)\frac{1-\exp(-\alpha\Delta x-s\Delta x/v_p-s\Delta x/v_n)}{(\alpha+s/v_p+s/v_n)v_p},\end{aligned}\tag{22}$$

$$\begin{aligned}N(x,s)&=N(x-\Delta x)\exp(-s\Delta x/v_n)\\&+N_{\rm e}(x-\Delta x)\exp(-s\Delta x/v_n)\{1-\exp(-\alpha\Delta x)\}\\&+\beta v_pP_{\rm e}(x)\frac{1-\exp(-\beta\Delta x-s\Delta x/v_p-s\Delta x/v_n)}{(\beta+s/v_p+s/v_n)v_n}.\end{aligned}\tag{23}$$

As mentioned above, we assume that the energy of carriers after ionization is zero. Therefore, the discrete expressions of Eq. (22) are given by

$$\begin{aligned}P(i,1)&=2\sum_{j'\geqslant j_{\rm ionh}}P(i+1,j')\exp(-s\Delta x/v_p)\\&\times\{1-\exp(-\beta(i+1)\Delta x)\}\\&+\alpha(i)v_n\sum_{j'\geqslant j_{\rm ionh}}N(i,j')\\&\times\frac{1-\exp(-\alpha(i)\Delta x-s\Delta x/v_p-s\Delta x/v_n)}{(\alpha(i)+s/v_p+s/v_n)v_p},\end{aligned}\tag{24}$$

$$P(i,\ j)=P(i+1,\ j-1)\exp(-s\Delta x/v_p).\tag{25}$$

Equation (25) shows that the holes cannot ionize and only be accelerated by the electric field. If $j-1$ reaches the threshold energy, then the first term of Eq. (25) will be multiplied by $\exp(-\beta(i+1)\Delta x)$. Similarly, the discrete expressions of Eq. (23) are given by

$$N(i,1)=2\sum_{j'\geqslant j_{\mathrm{ione}}}N(i-1,j')\exp(-s\Delta x/v_n)\times\{1-\exp(-\alpha(i-1)\Delta x)\}+\beta(i)v_p\sum_{j'\geqslant j_{\mathrm{ionh}}}P(i,j')\times\frac{1-\exp(-\beta(i)\Delta x-s\Delta x/v_p-s\Delta x/v_n)}{(\beta(i)+s/v_p+s/v_n)v_n},\quad(26)$$

$$N(i,j)=N(i-1,j-1)\exp(-s\Delta x/v_n).\quad(27)$$

And if $j-1$ reaches the threshold energy, then the first term of Eq. (27) will be multiplied by $\exp(-\alpha(i-1)\Delta x)$. Where i and j are space position and the energy state of the carriers, j_{ionh} is the value of j corresponding to the threshold energy level of holes, and j_{ione} is the value of j corresponding to the threshold energy level of electrons. The sum of the carrier density in the multiplication layer are given by

$$S_{P_{\mathrm{m}}}(x_{\mathrm{m}},s)=\sum_i\sum_j P(i,j)\Delta x,\quad(28)$$

$$S_{N_{\mathrm{m}}}(x_{\mathrm{m}},s)=\sum_i\sum_j N(i,j)\Delta x.\quad(29)$$

According to the boundary conditions, the loop iterations of Eqs. (24), (25), (26) and (27) are carried out until convergence. The procedure for computing $P(i,j)$ and $N(i,j)$ is the same as that in Ref. [15]. There is a difference in the boundary conditions, which are $N(1,j)=0$, $P(K_{\mathrm{max}},1)=P(x_{\mathrm{m}},s)$, and $P(K_{\mathrm{max}},j)=0$ for other j.

The dc gain is calculated from the ratio of the dc current (I) with ionization to that without ionization. The expression is given by

$$G_{\mathrm{dc}}=I(0)_{\mathrm{ionization}}/I(0)_{\mathrm{without-ionization}},\quad(30)$$

where “0” presents that the frequency is zero.

To get a more reasonable relation for the frequency response of the detector, it is necessary to consider the parasitic effects, and then we have

$$B=20\log_{10}\left(\frac{I(f)_{\mathrm{ionization}}}{I(0)_{\mathrm{ionization}}}H\right),\quad(31)$$

where f represents 3-dB bandwidth of the whole device when B is equal to –3, and H is the transfer function of the parasitic network, and then we have

$$H=\frac{1}{1+\mathrm{j}2\pi fRC}.\quad(32)$$

In Eq. (32), R is the sum of the series resistance and the load resistance. Also C, the junction capacitance of APD, is given by

$$\frac{1}{C}=\sum_i\frac{1}{C_i},\ C_i=\frac{\varepsilon_0\varepsilon_i}{x_i}A,\quad(33)$$

while C_i is the capacitance of a specified layer i, whose thickness is x_i and has a relative permittivity of ε_i in depletion layer, A is the area of the APD.

Taking account of temperature dependence for dead space theory, we adopt a temperature dependent ionization coefficient from the work of Okuto and Crowell [16] and the related work [17],

$$\alpha,\beta=\left(\frac{qF}{E_i}\right)\exp\left(0.217\left(\frac{E_i}{E_r}\right)^{1.14}-\left\{\left[0.217\left(\frac{E_i}{E_r}\right)^{1.14}\right]^2+\left(\frac{E_i}{qF\lambda}\right)^2\right\}^{1/2}\right),\quad(34)$$

where

$$E_r=E_{r0}\tanh(E_{r0}/2KT),\ \lambda=\lambda_0\tanh(E_{r0}/2KT).\quad(35)$$

In Eqs. (34) and (35), F denotes electric field, K denotes Boltzmann constant, T denotes temperature in Kelvins, λ denotes the mean free path, E_r denotes the average energy loss from scattering of each phonon, and E_i denotes the ionization threshold energy of carriers. E_{r0} and λ_0 denote the corresponding parameters under the temperature of 0 K. The relationship between the ionization threshold energy and the temperature is shown as follows.

$$E_i(T)=\frac{E_i(300\ \mathrm{K})}{E_{\mathrm{g}}(300\ \mathrm{K})}E_{\mathrm{g}}(T),\quad(36)$$

where the change of the band gap with the temperature can be expressed as following

$$E_{\mathrm{g}}(T)=1.421-\frac{3.63\times10^{-4}T^2}{T+162}.\quad(37)$$

3 Results and discussion

Figure 2(a) shows the simulation on basis of the proposed temperature dependent dead space theory, and the solid line denotes the linear fit. In contrast, in Fig. 2(b), it is demonstrated our previous reported experiments [18] and corresponding linear fit of the breakdown voltage changing with temperature for the InP/InGaAs SAGCM-APD. It is revealed from Fig. 2 that the theoretical temperature coefficient is 87.39 mV/K, while the temperature coefficient deduced from the experimental measurement is 90 mV/K [18].

An empirical formula for temperature coefficient has been reported [11], which is shown as following

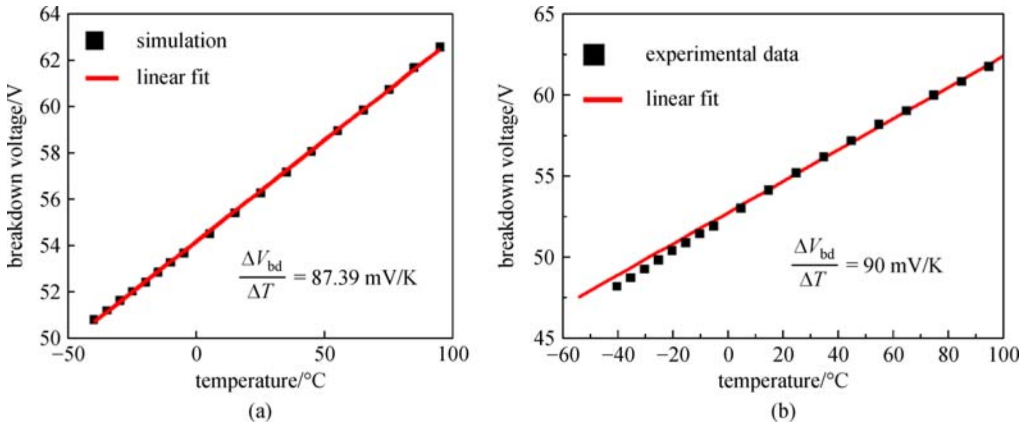

Fig. 2 (a) Simulation of breakdown voltage on basis of the proposed temperature dependent dead space model, and the solid line denotes the linear fit; (b) experimental data and the linear fit of breakdown voltage vs temperature

$$\frac{\Delta V_d}{\Delta T} = [(42.5 \times X_m) + 0.5] \times \frac{w}{X_m}, \tag{38}$$

where X_m denotes the width of the multiplication layer, and w denote the width for the whole depletion layer.

According to the empirical formula, the calculated temperature coefficient is 114.39 mV/K, which is much larger than our experiment, 90 mV/K as discussed above. A comparison of temperature coefficient from temperature dependent dead space theory, the empirical formula and experimental data reveals that the proposed temperature dependent dead space theory is believable, at least to our experimental results.

Figure 3(a) shows the 3 dB bandwidth for the InP/InGaAs SAGCM-APD vs multiplication. And the variation of the bandwidth with temperature at gain of 10 is also illustrated in Fig. 3(b). In Fig. 3(a), as expected, the bandwidth decreases as gain increases. The gain of the APD, as shown in Fig. 3(a), due to the thin multiplication layer (0.4 μm or so), is too low to be used as a SPAD. It is an inherent trade-off between gain and bandwidth for APDs, which is a bottleneck preventing APDs from being applied in traditional high speed communication and quantum communication simultaneously. In Figs. 3(a) and 3(b), the blue open circles denote the experimental data, which are consistent with the theory prediction. As revealed in Fig. 3(b), the bandwidth at a gain of 10 decreases with the increase of temperature, and shows a linear characteristic at a higher temperature region, and a small deviation in the low temperature region. This indicates that the decrease of the temperature in the high temperature region can effectively increase the bandwidth, but when the temperature drops to a certain value, the bandwidth tend to be saturated. The fitting coefficient of the relationship between bandwidth and temperature is 11.02 MHz/K. This may result from ionization coefficient,

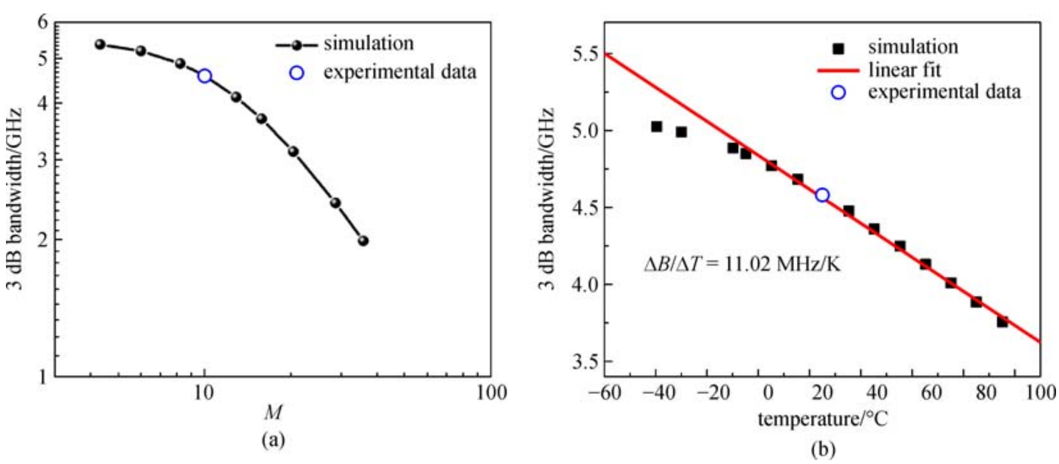

Fig. 3 (a) Simulation of 3 dB bandwidth vs multiplication on basis of the proposed temperature dependent dead space theory; (b) simulation of 3 dB bandwidth vs temperature on basis of the proposed temperature dependent dead space model, and the blue open circles denote the experimental data

band gap and drift velocity changing with temperature. The consistence of simulation with measurements further prove that our proposed model is reliable.

4 Conclusions

Based on the temperature dependent dead space model, the breakdown voltage and bandwidth of InP/InGaAs APD have been investigated theoretically and experimentally. The low temperature coefficient of 90 mV/K, as well as its consistence of the proposed model with experiments results, prove that the fabricated APD and our proposed temperature dependent dead space model are reliable. It is a trade-off between gain and bandwidth for APDs, which is a future work to pave a way for APDs applied in traditional high speed optical communication and SPAD for quantum communication simultaneously.

Acknowledgements This work was supported by the National Hi-Tech Research and Development Program of China (No. 2008AA1Z207), Natural Science Foundation of Hubei Province, China (No. 2010CDB01606), Fundamental Research Funds for the Central Universities (HUST: 2016YXMS027), Huawei Innovation Research Program (Nos. YJCB2010032NW, YB2012120133, YB2014010026 and YB2016040002), and Scientific Research Foundation for the Returned Overseas Chinese Scholars.

References

1. Campbell J C. Recent advances in telecommunications avalanche photodiodes. Journal of Lightwave Technology, 2007, 25(1): 109–121
2. Namekata N, Adachi S, Inoue S. 1.5 GHz single-photon detection at telecommunication wavelengths using sinusoidally gated InGaAs/InP avalanche photodiode. Optics Express, 2009, 17(8): 6275–6282
3. Wu G, Jian Y, Wu E, Zeng H. Photon-number-resolving detection based on InGaAs/InP avalanche photodiode in the sub-saturated mode. Optics Express, 2009, 17(21): 18782–18787
4. Namekata N, Sasamori S, Inoue S. 800 MHz single-photon detection at 1550-nm using an InGaAs/InP avalanche photodiode operated with a sine wave gating. Optics Express, 2006, 14(21): 10043–10049
5. Dixon A R, Dynes J F, Yuan Z L, Sharpe A W, Bennett A J, Shields A J. Ultrashort dead time of photon-counting InGaAs avalanche photodiodes. Applied Physics Letters, 2009, 94(23): 231113-1–231113-3
6. Bennett C H, Bessette F, Brassard G, Salvail L, Smolin J. Experimental quantum cryptography. Journal of Cryptology, 1992, 5(1): 3–28
7. Zhang J, Itzler M A, Zbinden H,Pan J W.Advances in InGaAs/InP single-photon detector systems for quantum communication. Light: Science and Applications, 2015, 4 (5): e286-1–e286-13
8. Hyun K S, Park C Y. Breakdown characteristics in InP/InGaAs avalanche photodiode with p-i-n multiplication layer structure. Journal of Applied Physics, 1997, 81(2): 974–984
9. Bandyopadhyay A, Jamal Deen M, Tarof L E, Clark W. A simplified approach to time-domain modeling of avalanche photodiodes. IEEE Journal of Quantum Electronics, 1998, 34(4): 691–699
10. Xie J, Ng J S, Tan C H. An InGaAs/AlAsSb avalanche photodiode with a small temperature coefficient of breakdown. IEEE Photonics Journal, 2013, 5(4): 6800706
11. Tan L J J, Ong D S G, Ng J S, Tan C H, Jones S K, Qian Y, David J P R. Temperature dependence of avalanche breakdown in InP and InAlAs. IEEE Journal of Quantum Electronics, 2010, 46(8): 1153–1157
12. Xiang J, Zhao Y. Comparison of waveguide avalanche photodiodes with InP and InAlAs multiplication layer for 25 Gb/s operation. Optical Engineering (Redondo Beach, Calif.), 2014, 53(4): 046106-1–046106-7
13. Zhao Y, He S. Multiplication characteristics of InP/InGaAs avalanche photodiodes with a thicker charge layer. Optics Communications, 2006, 265(2): 476–480
14. El-Batawy Y M, Deen M J. Analysis and circuit modeling of waveguide-separated absorption charge multiplication-avalanche photodetector (WG-SACM-APD). IEEE Transactions on Electron Devices, 2005, 52(3): 335–344
15. Das N R, Deen M J. On the frequency response of a resonant-cavity-enhanced separate absorption, grading, charge, and multiplication avalanche photodiode. Journal of Applied Physics, 2002, 92(12): 7133–7145
16. Okuto Y, Crowell C R. Energy-conservation considerations in the characterization of impact ionization in semiconductors. Physical Review B: Condensed Matter and Materials Physics, 1972, 6(8): 3076–3081
17. Chau H F, Pavlidis D. Physics based fitting and extrapolation method for measured impact ionization coefficients in III–V semiconductors. Journal of Applied Physics, 1992, 72(2): 531–538
18. Zhao Y, Zhang D, Qin L, Tang Q, Wu R H, Liu J, Zhang Y, Zhang H, Yuan X, Liu W. InGaAs-InP avalanche photodiodes with dark current limited by generation-recombination. Optics Express, 2011, 19(9): 8546–8556

Dr. **Yanli Zhao** graduated from Zhejiang University in 2002. He is currently a Professor at Huazhong University of Science and Technology, where he has been engaged in optical devices and their integration.

Junjie Tu, Ph.D. candidate in the Wuhan National Laboratory for Optoelectronics, Huazhong University of Science and Technology. Currently, his research interests are involved in high speed optical communication and photodevices.

Jingjing Xiang got master degree from Huazhong University of Science and Technology, majoring in the physical model for frequency response of APD including the dead space effect. From 2014 to present, she works for China Unicom Network Communications Co., Ltd as a Solution Manager.

Wen Ke, Ph.D. candidate in the Wuhan National Laboratory for Optoelectronics, Huazhong University of Science and Technology. Currently, his research interests are involved in high speed optical communication and photodevices.

Jing Xu, Ph.D. candidate in the Wuhan National Laboratory for Optoelectronics, Huazhong University of Science and Technology. Her current research interests include nanophotonics and integrated photonics.

Yang Tian is currently working toward the Ph.D. degree from Wuhan National Laboratory for Optoelectronics. His current research interest is infrared detectors.

Qian Li, Ph.D. candidate in the Wuhan National Laboratory for Optoelectronics, Huazhong University of Science and Technology. Currently, his research interests are involved in high speed optical communication and photodevices.

Yuchong Tian, M.S. candidate. His current research interests include integrated circuit design and optical device packaging.

Runqi Wang is currently a graduate student in Huazhong University of Science and Technology, where he has been engaged in optical device integration and packaging.

Wenyang Li received the B.S. degree from the South Central University for Nationalities, Wuhan, Hubei, China in 2013, and the M.S. degree from the Zhengzhou University, Zhengzhou, Henan, China in 2016. She is currently working toward the Ph.D. degree in the Wuhan National Laboratory for Optoelectronics, Huazhong University of Science and Technology, Wuhan, Hubei, China. Her current research interests include high-speed and high-power photodetectors.

Mingwei Guo is currently a candidate for the Ph.D. of Electronic Science and Technology in the National Optical and Electronic laboratory in Huazhong University of Science and Technology, who mainly focus on high speed PIN and APD, including some frontier integrated device like SOA-PIN, etc.

Zhifeng liu graduated as a master who majors in optical engineering from Zhengzhou University in April at 2010. From then on, he has been in engaging in researching in photodetector based on InP-substrate. Now, he is an employee in Aroptics-tech. Ltd.

Qi Tang, got master degree in Huazhong University of Science and Technology, majoring in optical engineering. Now, he works for Aroptics-tech. Ltd as General Manager.